Dynamic scaling and aging phenomena in a short-range Ising spin glass: $Cu_{0.5}Co_{0.5}Cl_2$-$FeCl_3$ graphite bi-intercalation compound

Itsuko S. Suzuki* and Masatsugu Suzuki†
Department of Physics, State University of New York at Binghamton, Binghamton, New York 13902-6016, USA
(Received 22 January 2003; revised manuscript received 1 April 2003; published 23 September 2003)

Static and dynamic behavior of short-range Ising spin glass (SG) $Cu_{0.5}Co_{0.5}Cl_2$-$FeCl_3$ graphite bi-intercalation compounds has been studied with superconducting quantum interference device dc and ac magnetic susceptibility. The T dependence of the zero-field relaxation time τ above a spin-freezing temperature $T_g(=3.92\pm0.11$ K) is well described by critical slowing down. The absorption χ'' below T_g decreases with increasing angular frequency ω, which is in contrast to the case of 3D Ising spin glass. The dynamic freezing temperature $T_f(H,\omega)$ at which $dM_{FC}(T,H)/dH=\chi'(T,H=0,\omega)$ is determined as a function of frequency (0.01 Hz $\leqslant\omega/2\pi\leqslant1$ kHz) and magnetic field ($0\leqslant H\leqslant5$ kOe). The dynamic scaling analysis of the relaxation time $\tau(T,H)$ defined as $\tau=1/\omega$ at $T=T_f(H,\omega)$ suggests the absence of SG phase in the presence of H (at least above 100 Oe). Dynamic scaling analysis of $\chi''(T,\omega)$ and $\tau(T,H)$ near T_g leads to the critical exponents ($\beta=0.36\pm0.03$, $\gamma=3.5\pm0.4$, $\nu=1.4\pm0.2$, $z=6.6\pm1.2$, $\psi=0.24\pm0.02$, and $\theta=0.13\pm0.02$). The aging phenomenon is studied through the absorption $\chi''(\omega,t)$ below T_g. It obeys a $(\omega t)^{-b''}$ power-law decay with an exponent $b''\approx0.15$–0.2. The rejuvenation effect is also observed under sufficiently large (temperature and magnetic-field) perturbations.

DOI: 10.1103/PhysRevB.68.094424 PACS number(s): 75.50.Lk, 75.40.Gb, 75.40.Cx

I. INTRODUCTION

In recent years there has been much effort to understand phase transitions of three-dimensional (3D) Ising spin glasses (SG's) with short-range interactions. The dynamic behavior of the low temperature SG phase has been a subject of some controversy. There are basically two different pictures of the SG phase, the mean-field picture (including Monte Carlo simulations)[1] and the scaling picture.[2–7]

The mean-field picture is originated from the replica-symmetry-breaking solution of Parisi for the infinite-range Sherrington-Kirkpatrick model.[1] In this picture the SG phase has a complicated free-energy structure with a number of degenerate minimum separated with each other by large free-energy barriers. The SG phase survives in the presence of a magnetic field. A de Almeida-Thouless line separates the SG phase from a paramagnetic phase.[8]

The scaling picture (so-called the droplet model) is based on renormalization group arguments.[2–7] In this picture there are only two thermodynamic states related to each other by a global spin flip, and the important excitations at low temperatures are droplets of overturned spins. In three dimensions a true phase transition should exist only in zero field and no irreversibility should be seen in the presence of any finite magnetic field.

Because of extremely long relaxation time, there is no direct measurement available that can demonstrate whether the SG phase exists even in zero magnetic field.[9–11] The dynamic scaling analysis is required to overcome such an experimental difficulty in confirming the existence of thermally equilibrium SG phase in a finite magnetic field. This problem has been addressed by Mattsson *et al.*[9] They have studied the dynamic susceptibility of a 3D Ising SG, $Fe_{0.5}Mn_{0.5}TiO_3$. The in-field scaling behavior of the dynamic susceptibility, which is remarkably different from the zero-field behavior, is explained as demonstrating the absence of SG phase in a finite field.

In this paper we study the slow dynamics of the SG phase in a short-range 3D Ising SG, $Cu_{0.5}Co_{0.5}Cl_2$-$FeCl_3$ graphite bi-intercalation compound (GBIC), using superconducting quantum interference device (SQUID) dc and ac magnetic susceptibility. This compound undergoes a SG transition at a spin freezing temperature $T_g(=3.92\pm0.11$ K) at zero magnetic field. Following a method used by Mattsson *et al.*,[9] we determine the dynamic freezing temperature $T_f(H,\omega)$, at which $dM_{FC}(T,H)/dH=\chi'(T,H=0,\omega)$, as a function of frequency (0.01 Hz $\leqslant\omega/2\pi\leqslant1$ kHz) and field ($0\leqslant H\leqslant5$ kOe). The dynamic scaling analysis of the relaxation time $\tau(T,H)$ defined as $\tau=1/\omega$ at $T=T_f(H,\omega)$ suggests that the SG phase does not survive in the presence of H (at least above 100 Oe). The critical exponents are determined from the dynamic scaling analysis for $\chi''(T,\omega)$ and $\tau(T,H)$ and compared to those for $Fe_{0.5}Mn_{0.5}TiO_3$. The aging phenomenon is also studied through the time dependence of the absorption $\chi''(\omega,t)$ below T_g. It obeys a $(\omega t)^{-b''}$ power-law decay with an exponent $b''\approx0.15$–0.2.

$Cu_{0.5}Co_{0.5}Cl_2$-$FeCl_3$ GBIC has a unique layered structure where the $Cu_{0.5}Co_{0.5}Cl_2$ intercalate layer ($=I_1$) and $FeCl_3$ intercalate layers ($=I_2$) alternate with a single graphite layer (G), forming a stacking sequence ($\text{-}G\text{-}I_1\text{-}G\text{-}I_2\text{-}G\text{-}I_1\text{-}G\text{-}I_2\text{-}G\text{-}\cdot$) along the c axis.[12,13] In the $Cu_{0.5}Co_{0.5}Cl_2$ intercalate layer two kinds of magnetic ions (Cu^{2+} and Co^{2+}) are randomly distributed on the triangular lattice. The spin order in the $Cu_{0.5}Co_{0.5}Cl_2$ layers is coupled with that in the $FeCl_3$ intercalate layer through an interplanar exchange interaction, leading to the spin frustration effect.

The XY and Ising character of the present system are due to the easy-plane-type anisotropy field H_A^{out} and the in-plane anisotropy field H_A^{in}, respectively: $H_A^{out}\gg H_A^{in}$. Although the in-plane structure of $Cu_{0.5}Co_{0.5}Cl_2$ layers is incommensurate

with that of graphene sheets, Cu and Co atoms tend to sit over hexagon centers of graphene sheets because of the interplanar structural correlation. The sixfold symmetry of graphene sheets imposes the in-plane spin anisotropy in the *c* plane. Because of this, the spins tend to align along the easy axis with sixfold symmetry in the *c* plane.[14]

It is well known that the intercalate layers are formed of small islands in acceptor graphite intercalation compounds (GIC's).[14] In stage-2 $CoCl_2$ GIC, for example, there is a charge transfer from graphene sheets to the $CoCl_2$ intercalate layer. The periphery of such islands provides sites for charges transferred. The size of islands is on the order of 400 Å. In spite of few structural studies, it is predicted that similar island structures exist both in the $Cu_{0.5}Co_{0.5}Cl_2$ and $FeCl_3$ layers of our system.

II. EXPERIMENTAL PROCEDURE

A sample of stage-2 $Cu_{0.5}Co_{0.5}Cl_2$ GIC as a starting material was prepared from single crystal kish graphite (SCKG) by vapor reaction of anhydrated $Cu_{0.5}Co_{0.5}Cl_2$ in a chlorine atmosphere with a gas pressure of $\approx$740 Torr.[15,16] The reaction was continued at 500°C for three weeks. The sample of $Cu_{0.5}Co_{0.5}Cl_2$-$FeCl_3$ GBIC was prepared by a sequential intercalation method: the intercalant $FeCl_3$ was intercalated into empty graphite galleries of stage-2 $Cu_{0.5}Co_{0.5}Cl_2$ GIC. A mixture of well-defined stage-2 $Cu_{0.5}Co_{0.5}Cl_2$ GIC based on SCKG and single-crystal $FeCl_3$ was sealed in vacuum inside Pyrex glass tubing, and was kept at 330 °C for two weeks. The stoichiometry of the sample is represented by $C_m(Cu_{0.5}Co_{0.5}Cl_2)_{1-c}(FeCl_3)_c$. The concentration of C and Fe (m and c) was determined from weight uptake measurement and electron microprobe measurement [using a scanning electron microscope (Model Hitachi S-450)]: $m=5.26\pm0.05$ and $c=0.53\pm0.03$. The $(00L)$ x-ray diffraction measurements of stage-2 $Cu_{0.5}Co_{0.5}Cl_2$ GIC and $Cu_{0.5}Co_{0.5}Cl_2$-$FeCl_3$ GBIC were made at 300 K by using a Huber double circle diffractometer with a MoKα x-ray radiation source (1.5 kW). The *c*-axis repeat distance of stage-2 $Cu_{0.5}Co_{0.5}Cl_2$ GIC and $Cu_{0.5}Co_{0.5}Cl_2$-$FeCl_3$ GBIC was determined as 12.83 ± 0.05 Å and 18.81 ± 0.05 Å, respectively.

The dc magnetization and ac susceptibility were measured using a SQUID magnetometer (Quantum Design, MPMS XL-5) with an ultra low field capability option. First a remnant magnetic field was reduced to zero field (exactly less than 3 mOe) at 298 K for both dc magnetization and ac susceptibility measurements. Then the sample was cooled from 298 to 1.9 K in a zero field.

(i) *Measurements of the zero-field-cooled (ZFC) susceptibility* (χ_{ZFC}) *and the field-cooled (FC) susceptibility* (χ_{FC}). After an external magnetic field H ($0\leqslant H\leqslant 1$ kOe) was applied along the *c* plane (basal plane of graphene layer) at 1.9 K, χ_{ZFC} was measured with increasing temperature (T) from 1.9 to 20 K. After annealing of sample for 10 min at 50 K in the presence of H, χ_{FC} was measured with decreasing T from 20 to 1.9 K.

(ii) *AC susceptibility measurement.* The frequency (f), magnetic field, and temperature dependence of the dispersion (χ') and absorption (χ'') was measured between 1.9 and 20 K, where the frequency of the ac field is $f=0.01$–1000 Hz and the amplitude h is typically $h=50$ mOe.

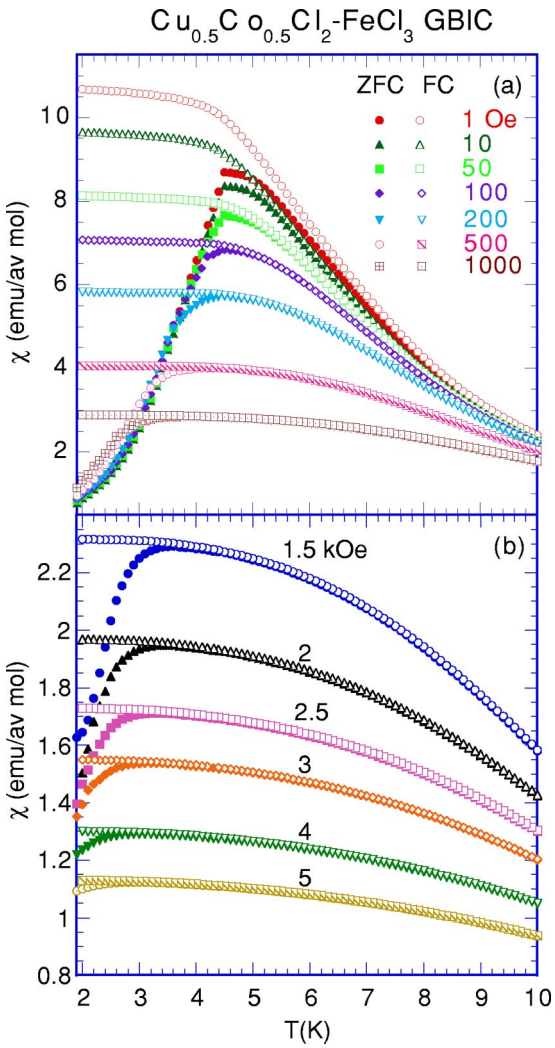

FIG. 1. (a) and (b) T dependence of χ_{ZFC} and χ_{FC} at various H for $Cu_{0.5}Co_{0.5}Cl_2$-$FeCl_3$ GBIC. H is applied along the *c* plane (graphene basal plane) perpendicular to the *c* axis.

III. RESULT

A. $\chi_{ZFC}(T,H)$ and $\chi_{FC}(T,H)$

Figures 1(a) and 1(b) show the T dependence of the ZFC and FC susceptibilities (χ_{ZFC} and χ_{FC}) of $Cu_{0.5}Co_{0.5}Cl_2$-$FeCl_3$ GBIC at various H, where the magnetic field (H) is applied along the *c* plane perpendicular to the *c* axis. The T dependence of χ_{ZFC} and χ_{FC} is similar to that of $Fe_{0.5}Mn_{0.5}TiO_3$.[17] The susceptibility χ_{ZFC} at $H=1$ Oe exhibits a cusp around 4.5 K, while χ_{FC} is nearly temperature independent below 3.9 K. Note that χ_{FC} along the *c* axis at $H=1$ Oe is on the order of one-tenth of χ_{FC} along the *c* plane around 3.9 K. Figure 2(a) shows the T dependence of the difference δ defined by $\delta=\chi_{FC}-\chi_{ZFC}$ at various H, which is the measure for the irreversibility of the susceptibility. The deviation of χ_{ZFC} from χ_{FC} at $H=1$ Oe starts to

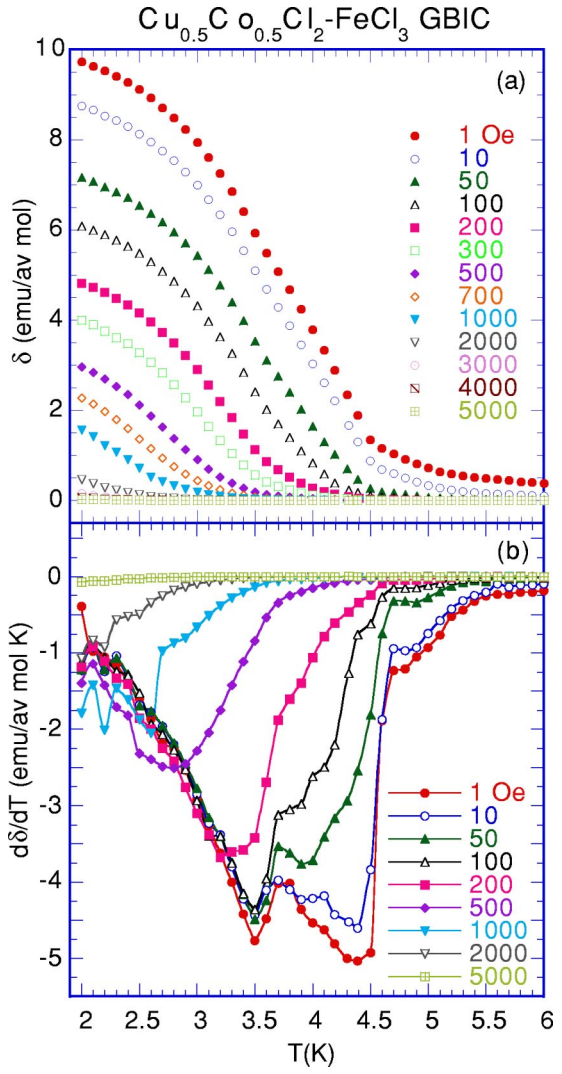

FIG. 2. T dependence of (a) $\delta(=\chi_{FC}-\chi_{ZFC})$ and (b) $d\delta/dT$ at various H. The value of δ is derived from Fig. 1. The solid lines are guides to the eyes.

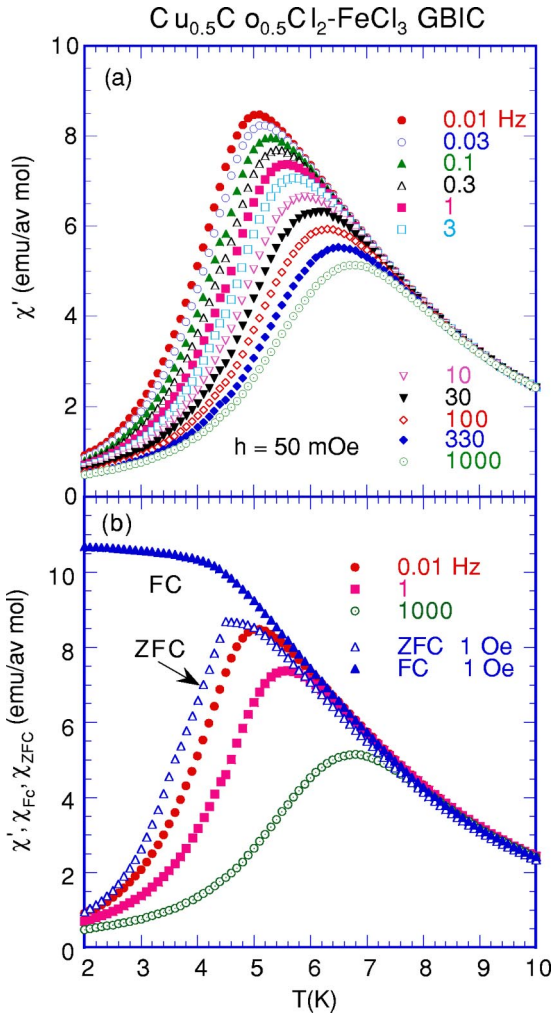

FIG. 3. (a) T dependence of χ' at various f. $h=50$ mOe. $H=0$. (b) T dependence of χ_{ZFC} and χ_{FC} ($H=1$ Oe), which is compared with that of χ' at $f=0.01$, 1, and 1000 Hz ($H=0$).

occur below 10 K, and drastically increases with decreasing T below the cusp temperature of χ_{ZFC}. The inflection-point temperature of δ vs T corresponds to a local minimum temperature of $d\delta/dT$ vs T, shown in Fig. 2(b). The inflection-point temperature of δ drastically decreases with increasing H, leading to the AT line in the (H,T) diagram (see Sec. III D for further discussion). The nonvanishing δ well above the inflection-point temperature is partly due to the islandic nature of $Cu_{0.5}Co_{0.5}Cl_2$ and $FeCl_3$ layers. The growth of the in-plane spin correlation length is partly limited by the existence of small islands, leading to the smearing of the inflection-point temperature over the system.

B. Relaxation time: $\chi'(T,\omega)$ and $\chi''(T,\omega)$

In Fig. 3(a) we show the T dependence of the dispersion $\chi'(T,\omega)$ at various frequencies ($f=0.01-1000$ Hz), where $\omega(=2\pi f)$ is the angular frequency and $h(=50$ mOe) is the amplitude of the ac field. In Fig. 3(b), the T dependence of χ_{ZFC} and χ_{FC} at $H=1$ Oe is compared to typical data of $\chi'(T,\omega)$. The susceptibility χ_{FC} may correspond to the equilibrium susceptibility (χ_{eq}). In Fig. 4(a) we show the T dependence of the absorption $\chi''(T,\omega)$ at various f. Similar behaviors in $\chi'(T,\omega)$ and $\chi''(T,\omega)$ have been observed in Fe-C nanoparticles by Hansen *et al.*[18] Figure 4(b) shows the T dependence of the derivative $d\chi''(T,\omega)/dT$. If we assume conventional critical slowing down on approaching the SG transition temperature T_g from the high-T side, the T dependence of the relaxation time τ can be described by[19]

$$\tau=\tau^*(T/T_g-1)^{-x}, \tag{1}$$

with $x=\nu z$, where z is the dynamic critical exponent, ν is the critical exponent of the spin correlation length ξ, and τ^* is the characteristic time. In the analysis of τ vs T, T corresponds to the local minimum temperature of $d\chi''/dT$ vs T, or the peak temperatures of χ'' vs T and χ' vs T, where τ is set equal to ω^{-1}. In Fig. 5 we show the T dependence of τ thus obtained. The least squares fits of the data of τ vs T yield $x=10.3\pm0.7$, $T_g=3.92\pm0.11$ K, $\tau^*=(5.27\pm0.07)\times10^{-6}$ sec for the local minimum temperature of $d\chi''/dT$ vs T, $x=15.5\pm1.5$, $T_g=2.98\pm0.18$ K, $\tau^*=(8.56\pm0.05)$

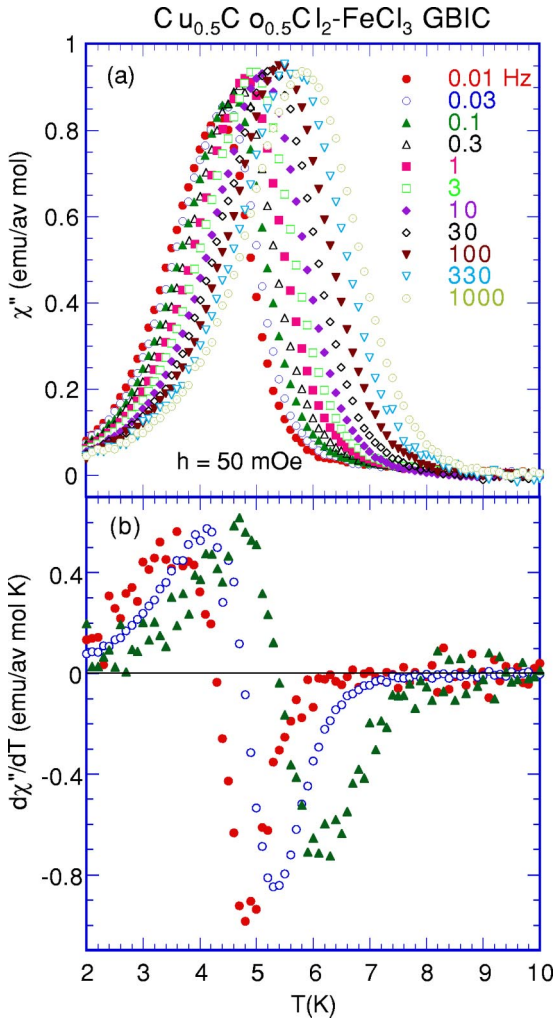

FIG. 4. T dependence of (a) χ'' and (b) $d\chi''/dT$ at various f; $h=50$ mOe, $H=0$.

$\times 10^{-5}$ sec for the peak temperature of χ'' vs T, and $x=15.3\pm2.0$, $T_g=3.57\pm0.27$ K, $\tau^*=(3.08\pm0.10)\times10^{-5}$ sec for the peak temperature of χ' vs T. The parameters thus obtained are rather different. The relaxation time τ^* is much larger than a microscopic relaxation time τ_0 (typically 10^{-10} sec). Here we assume that the local minimum temperature of $d\chi''/dT$ vs T at $\omega=0$ corresponds to the spin freezing temperature T_g. T_g is close to a temperature below which χ_{FC} at $H=1$ Oe becomes nearly constant. The value of $x(=10.3\pm0.7)$ is rather close to that predicted by Ogielski for the 3D $\pm J$ Ising SG ($x=7.9\pm1.0$) (Ref. 20) from Monte Carlo (MC) simulations. The situation is a little different for $Fe_{0.5}Mn_{0.5}TiO_3$.[19] In the analysis of τ vs T, T is determined either as the maximum of χ' or as the inflection point of χ''. In both cases, τ is well described by Eq. (1) with $T_g=20.95\pm0.1$ K, $x=10.0\pm1.0$, and $\log_{10}\tau_0=-12.8\pm1.0$, where τ_0 is a microscopic relaxation time. The value of x is in excellent agreement with our result.

Here we assume a generalized form of the relaxation time, more suitable to the description of SG behavior near T_g.[21] The relaxation time $\tau(l,T)$, which is needed to flip the

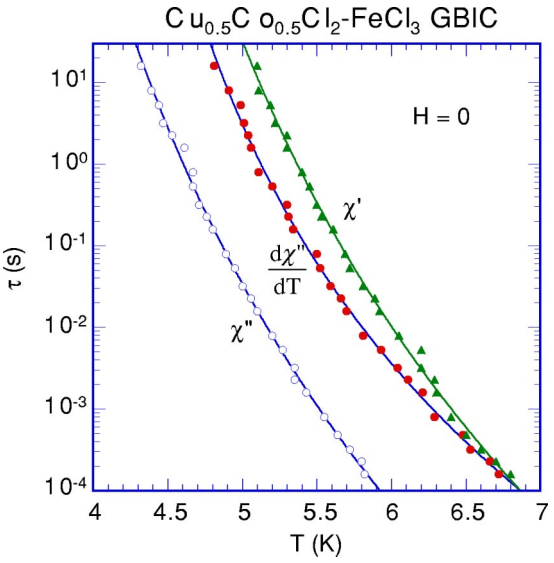

FIG. 5. T dependence of relaxation time τ, which is determined from peak temperatures of χ'' vs T and χ' vs T, and local minimum temperature of $d\chi''/dT$ vs T. The solid lines are fits to Eq. (1) (critical slowing down) with parameters x, T_g, and τ^* given in the text.

l-sized cluster of spins, is governed by thermal activation over a barrier $B_T(l)$, in such a way that

$$\tau(l,T)=\tau_0 l^z \exp[B_T(l)/k_BT], \tag{2}$$

where l is in units of the lattice constant a. The energy barrier is described by $B_T(l)=Y(T)l^{\psi}$, where ψ is the barrier exponent. The wall stiffness $Y(T)$ should vanish above T_g like in ferromagnets and is described by $Y(T)=Y_0(1-T/T_g)^{\psi\nu}$ below T_g, where ν is the critical exponent of spin correlation length ξ and Y_0 is on the order of k_BT_g. Above T_g the exponential term in Eq. (2) is nearly equal to 1, leading to the expression for the critical slowing down above T_g: $\tau_+(l,T)\approx\tau_0 l^z$.

C. Dynamic scaling of $T\chi''(T,\omega)$

Figures 6(a) and 6(b) show the f dependence of $\chi'(T,\omega)$ and $\chi''(T,\omega)$ at various T in the vicinity of $T_g(=3.92$ K), respectively. The absorption $\chi''(T,\omega)$ curves exhibit different characteristics depending on T. Above T_g, $\chi''(T,\omega)$ shows a peak at a characteristic frequency, shifting to the high f-side as T increases. Below T_g, $\chi''(T,\omega)$ shows no peak for $f\geqslant0.01$ Hz. It decreases with increasing f, following a power law $\omega^{-\alpha''}$. The exponent α'' is almost independent of T: $\alpha''=0.096\pm0.003$. According to the fluctuation-dissipation theorem, the magnetic fluctuation spectrum $S(\omega)$ is related to $\chi''(T,\omega)$ by $S(T,\omega)=2k_BT\chi''(T,\omega)/\omega$.[22] Then $S(T,\omega)$ is proportional to $\omega^{-(1+\alpha'')}$, which is similar to $1/\omega$ character of typical SG. In contrast, $\chi'(T,\omega)$ decreases with increasing f at any T near T_g: χ' exhibits a power law $\omega^{-\alpha'}$. The exponent α' is weakly dependent on T: $\alpha'=0.088\pm0.001$ at $T=3$ K and $\alpha'=0.111\pm0.001$ at $T=3.8$ K. The value of α' agrees well with that of α''. In fact, χ'' is

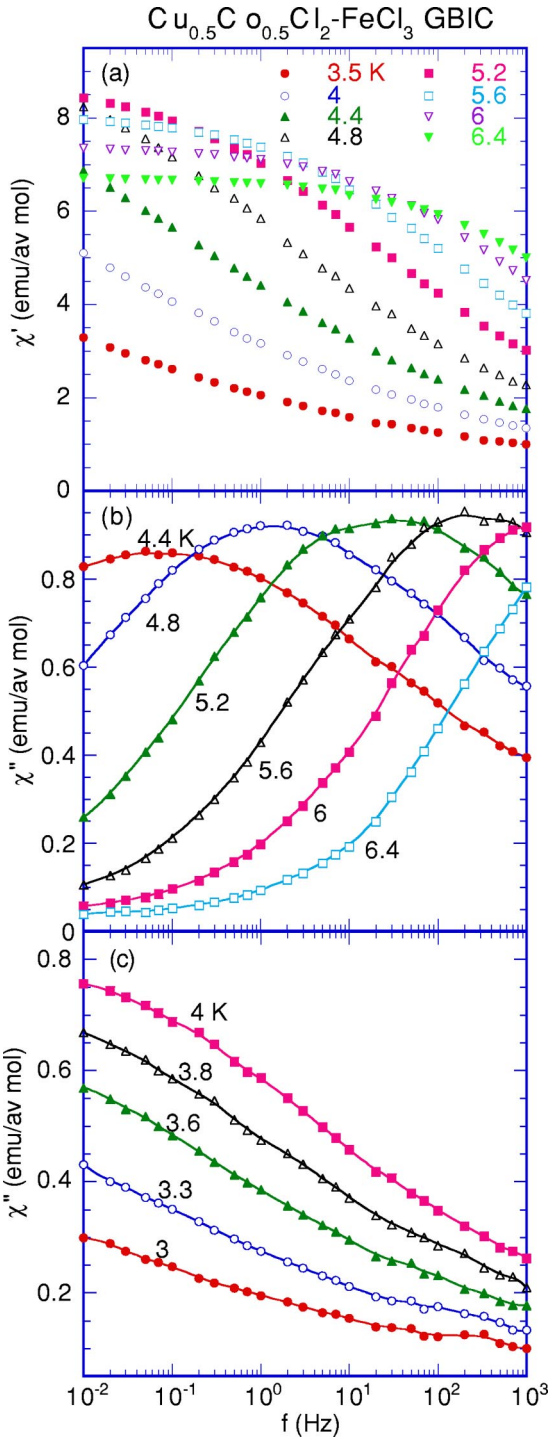

FIG. 6. (a) f dependence of χ' at various T; $H=0$ Oe. (b) and (c) f dependence of χ'' below and above T_g. $T_g=3.92$ K, $H=0$ Oe. The solid lines are guides to the eyes.

related to χ' through a so-called "$\pi/2$ rule:" $\chi''=-(\pi/2)d\chi'/d(\ln\omega)$ (Kramers-Kronig relation), leading to the relation $\alpha'=\alpha''$. Here we note that the observed f dependence of χ'' in $Cu_{0.5}Co_{0.5}Cl_2$-$FeCl_3$ GBIC is different from that in conventional spin glasses such as $Fe_{0.5}Mn_{0.5}TiO_3$ (Ref. 19) and $Eu_{0.4}Sr_{0.6}S$.[23] In these conventional spin glasses, χ'' increases with increasing f both above and below T_g.

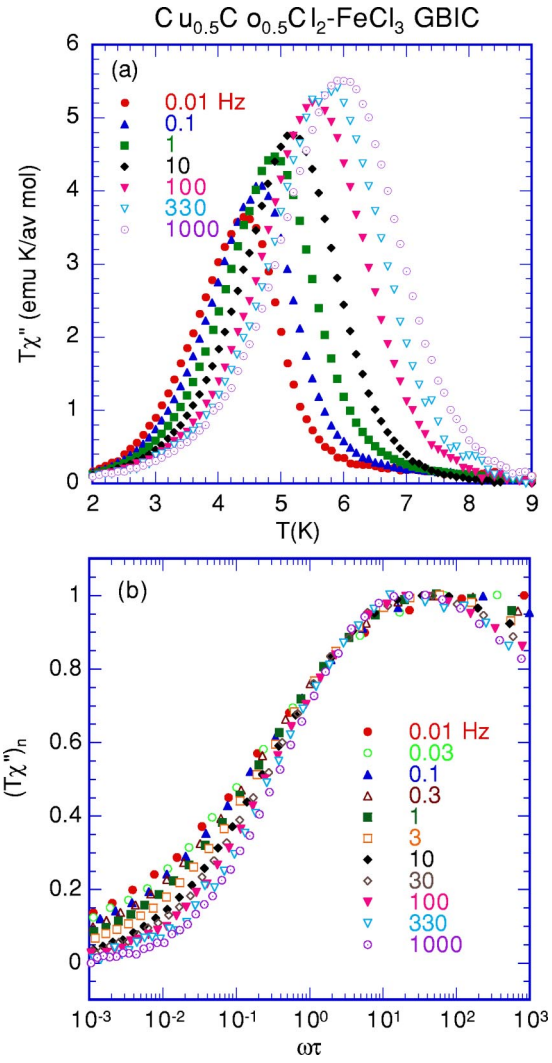

FIG. 7. (a) T dependence of $T\chi''$ at various f; $H=0$. (b) Scaling plot of $(T\chi'')_n$ $(=(T\chi'')/(T\chi'')_{max}$ as a function of $\omega\tau$. $(T\chi'')_{max}$ is the maximum value of $T\chi''$. The relaxation time τ is described by Eq. (1) with $x=10.3$, $T_g=3.92$ K, and $\tau^*=5.27\times10^{-6}$ sec.

We consider the validity of a dynamic scaling law for $T\chi''$, which is predicted to be described by[24]

$$T\chi''=\omega^y\Omega(\omega\tau), \tag{3}$$

where $\Omega(\omega\tau)$ is a scaling function of $\omega\tau$ and is assume to take a maximum at $\omega\tau=$constant. The value y $(=\beta/x)$ is a critical exponent, where β is a critical exponent of the order parameter (q). Figure 7(a) shows the T dependence of $T\chi''$ at various f. The curve of $T\chi''$ vs T exhibits a peak, which shifts to the high-T side as f increases. The peak height of $T\chi''$ defined by $(T\chi'')_{max}$ increases with increasing f. The least squares fit of the data for the peak height of $T\chi''$ vs ω (for $0.01\leqslant f\leqslant1000$ Hz) to the form of $\approx\omega^y$ yields $y=0.035\pm0.001$. Then the value of $\beta(=xy)$ is estimated as $\beta=0.36\pm0.03$, where $x=10.3\pm0.7$. This value of β is smaller than that $(\beta=0.54)$ for $Fe_{0.5}Mn_{0.5}TiO_3$.[25] Figure 7(b) shows the scaling plot of $(T\chi'')_n=(T\chi'')/(T\chi'')_{max}$ as a function of $\omega\tau$, where τ is given by Eq. (1) with $x=10.3$,

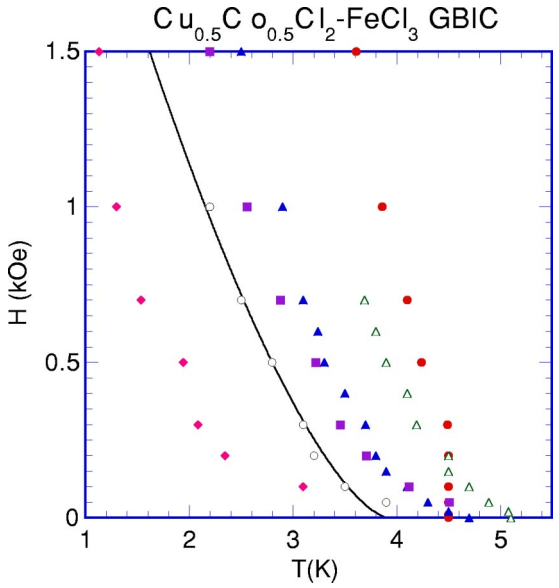

FIG. 8. H-T phase diagram, where the peak temperatures of χ_{ZFC} vs T (●), $d\chi''(T,H,f=0.1\ \text{Hz})/dT$ vs T (△), $\chi''(T,H,f=0.1\ \text{Hz})$ vs T (▲), and the local minimum temperature of $d\delta/dT$ vs T (○). For comparison, $T_f(H,\omega)$ with $f=0.01$ Hz (■) [see also Fig. 12(a)] and $T_f(H)$ (◆) [see Eq. (8) and Fig. 14 for definition] are shown as a function of H. The solid lines are the fits of the data (see text).

$T_g=3.92$ K, $\tau^*=5.27\times10^{-6}$ sec. In this plot the data $\chi''(T,H=0,\omega)$ for $4\leqslant T\leqslant 10$ K and 0.01 Hz$\leqslant f\leqslant 1$ kHz are used. It seems that the data points fit well with a scaling function $\Omega(\omega\tau)$, indicating the validity of the dynamic scaling law given by Eq. (3).

D. Possibility of AT line determined from $d\delta/dT$ vs T

According to the AT theory,[8] it is predicted that an ideal SG system in the presence of H undergoes a SG transition at the spin-freezing temperature $T_f(H)$ in the (H,T) plane. The deviation of χ_{ZFC} from χ_{FC} starts to occur for $T<T_f(H)$. Experimentally it is a little difficult to determine exactly the line $T_f(H)$ at which $\delta=\chi_{FC}-\chi_{ZFC}=0$ because of possible distribution of $T_f(H)$ arising from the islandic nature of the system. Instead, we use another definition for the line $T_f(H)$ at which $d\delta/dT$ vs T exhibits a local minimum at each H [see Fig. 2(b)]. In Fig. 8 we show the line $T_f(H)$ thus obtained (the local minimum temperatures of $d\delta/dT$ vs T) in the (H,T) plane. For comparison, we also plot the peak temperatures of $\chi_{ZFC}(T,H)$ vs T, $\chi''(T,H,\omega)$ vs T at $f=0.1$ Hz, and the local minimum temperature of $d\chi''(T,H,\omega)/dT$ vs T with $f=0.1$ Hz as a function of H in the (H,T) plane. Note that the data of $\chi''(T,H,\omega)$ vs T at $f=0.1$ Hz will be given later (see Fig. 9). These lines are away from the line $T_f(H)$. The least squares fit of the data of the line $T_f(H)$ for 100 Oe $\leqslant H\leqslant 1$ kOe to

$$H=H_0[1-T_f(H)/T_g]^p \tag{4}$$

yields parameters $p=1.52\pm0.10$ and $H_0=3.4\pm0.4$ kOe, where $T_g=3.92\pm0.11$ K. In the mean-field picture,[1,8] this line corresponds to the AT line. In fact, the value of exponent p is close to that ($p=1.50$) for the AT line.

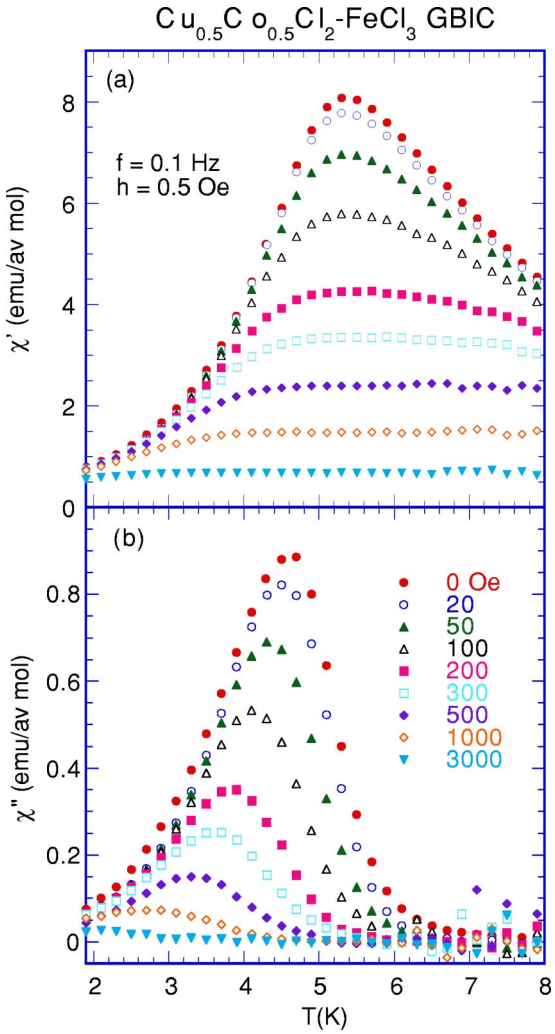

FIG. 9. T dependence of (a) χ' and (b) χ'' at various H; $f=0.1$ Hz and $h=0.5$ Oe.

It has been believed that the mean-field picture is valid for $Fe_{0.5}Mn_{0.5}TiO_3$: $p=1.49$.[26] However, Mattsson *et al.*[9] have claimed that the SG transition is destroyed by the application of a finite magnetic field H in $Fe_{0.5}Mn_{0.5}TiO_3$. Their result supports the prediction from the scaling picture that the long-range SG order at equilibrium only occurs for $H=0$ and $T<T_g$. Further discussion for the AT line will be done in Secs. III E and III F.

E. Effect of H on the SG transition

The transition from the paramagnetic phase to the SG phase occurs in our system at $H=0$. What happens to this transition in the presence of H? Does the long-range SG phase survive as suggested by the molecular field picture or is destroyed as suggested by the scaling picture? According to the method developed by Mattsson *et al.*,[9] here we have determined the dynamic freezing temperature $T_f(H,\omega)$ in a wide frequency and field interval. Figure 9 shows the T dependence of $\chi'(T,H,\omega)$ and $\chi''(T,H,\omega)$ at various H for f

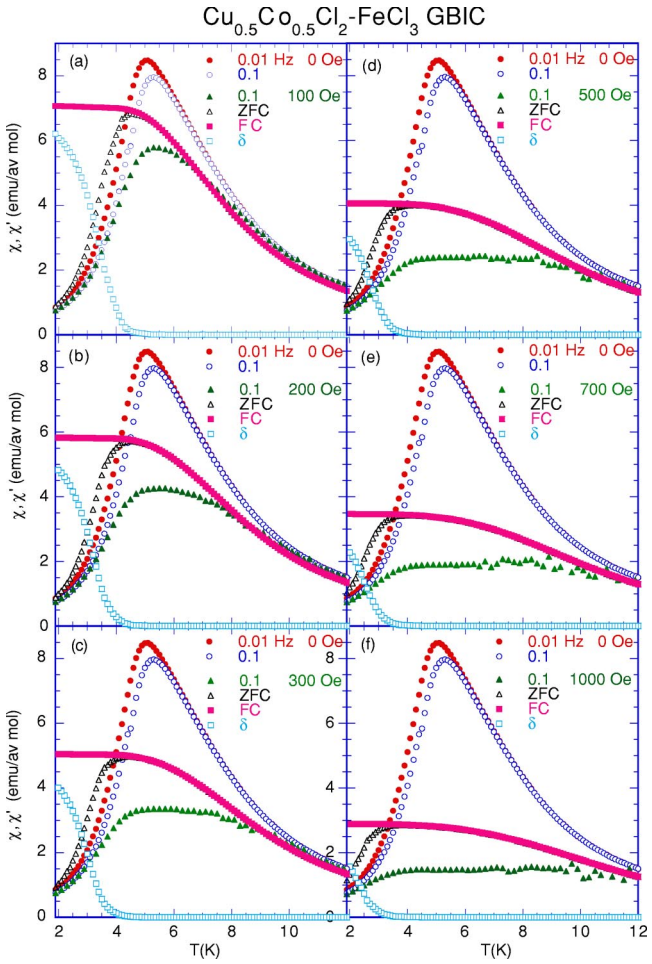

FIG. 10. (a)–(f) T dependence of χ' at $f=0.01$ and 0.1 Hz ($H=0$), χ' at $f=0.1$ Hz at H, χ_{ZFC}, χ_{FC}, and $\delta(=\chi_{FC}-\chi_{ZFC})$ at the same H. $H=100$, 200, 300, 500, 700, and 1000 Oe.

$=\omega/2\pi=0.1$ Hz, where $h=0.5$ Oe and $H(0<H\leqslant 3$ kOe) is applied along the c plane perpendicular to the c axis. In Figs. 10(a)–(f), we show the T dependence of $\chi'(T,H=0,\omega)$ at $f=0.01$ and 0.1 Hz, $\chi'(T,H,\omega)$ at $f=0.1$ Hz, $\chi_{FC}(T,H)$, $\chi_{ZFC}(T,H)$, and $\delta=\chi_{FC}(T,H)-\chi_{ZFC}(T,H)$ at various $H=100$–1000 Oe. The susceptibility $\chi_{FC}(T,H)(=M_{FC}/H)$ corresponds to the equilibrium susceptibility. Since $M_{FC}(T,H)$ is a nonlinear function of H, $\chi_{FC}(=M_{FC}/H)$ is not equal to the differential FC susceptibility dM_{FC}/dH. The numerical calculations indicate that dM_{FC}/dH is smaller than χ_{FC} at the same H and T. In Fig. 11 we show the T dependence of $dM_{FC}(T,H)/dH$ at various H and $\chi'(T,H=0,\omega)$ at various f. The spin-freezing temperature $T_f(H,\omega)$ is defined as a temperature at which $dM_{FC}(T,H)/dH$ coincides with $\chi'(T,H=0,\omega)$. As shown in Fig. 10, $\chi'(T,H,\omega)$ at $f=0.1$ Hz deviates from $\chi'(T,H=0,\omega)$ at the same f above $T_f(H,\omega)$. This is the same method that has been used by Mattsson *et al.*[9] to obtain $T_f(H,\omega)$ for $Fe_{0.5}Mn_{0.5}TiO_3$. The advantage of this method is that we do not have to measure the T dependence of χ' and χ'' at each H such as the data shown in Fig. 9. In Fig. 12(a) we show a plot of the line $T_f(H,\omega)$ in the (H,T) plane, where f ($0.01\leqslant f\leqslant 1000$ Hz) is varied as a parameter.

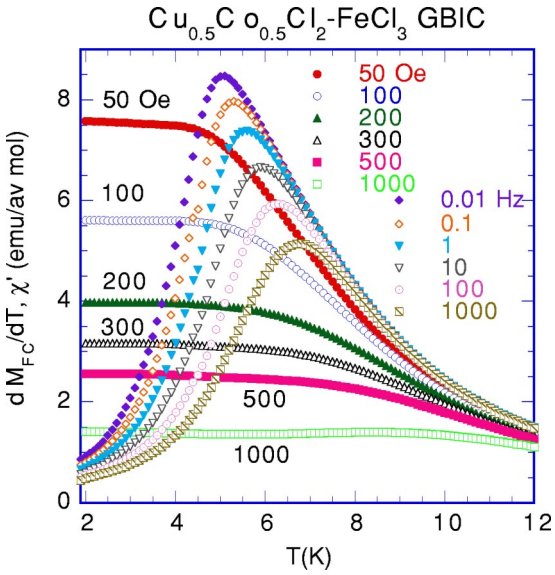

FIG. 11. T dependence of $\chi'(T,H=0,\omega)$ and $dM_{FC}(T,H)/dH$. The spin-freezing temperature $T_f(H,\omega)$ is defined by a temperature at which $\chi'(T,H=0,\omega)$ is equal to $dM_{FC}(T,H)/dH$.

For comparison, the line $T_f(H,\omega)$ at $f=0.01$ Hz is also plotted in the H-T diagram of Fig. 8. We find that this line is close to the line $T_f(H)$ determined from the local minimum temperature of $d\delta/dT$ vs T. This result suggests that the method to determine $T_f(H,\omega)$ is appropriate. Note that similar data of $T_f(H,\omega)$ has been reported by Mattsson *et al.* for $Fe_{0.5}Mn_{0.5}TiO_3$.[9] Figure 12(b) shows the T dependence of $\tau(T,H)$, which is derived from Fig. 12(a); $\tau(T,H)=1/\omega=1/(2\pi f)$ at $T=T_f(H,\omega)$.

Assuming a SG phase transition at T_g, we assume the following dynamic scaling relation for the relaxation time $\tau_{\pm}(T,H)$ in the presence of H:[27]

$$\tau_{\pm}(T,H)=|\epsilon|^{-x}F_{\pm}(X)=H^{-2x/(\beta+\gamma)}G_{\pm}(X) \qquad (5)$$

with $X=|\epsilon|H^{-2/(\beta+\gamma)}$, where $(+)$ denotes $T>T_g$ and $(-)$ denotes $T<T_g$, ϵ is the reduced temperature defined by $\epsilon=T/T_g-1$, $\tau_c\approx\tau_0|\epsilon|^{-x}$ is the relaxation time for $T>T_g$ at $H=0$, γ is the exponent of nonlinear dynamic susceptibility χ_3, F_+ and G_+ are the scaling functions for $T>T_g$ and F_- and G_- are those for $T<T_g$. The scaling relation, Eq. (5), suggests that τ diverges like $\tau(T=T_g,H)\approx H^{-2x/(\beta+\gamma)}$ as $H\to 0$. The characteristic field denoted by $H^*\approx|\epsilon|^{(\beta+\gamma)/2}$ is a crossover line between a weak-field and a strong-field region for $T>T_g$.

In the scaling picture, the asymptotic form for τ_- below T_g is obtained as follows. In Eq. (2) we assume that l diverges like $l\approx H^{-2/(d-2\theta)}$ as H reduces to zero.[5] Then τ_- can be rewritten as

$$\tau_-(T,H)\approx H^{-2z/(d-2\theta)}\exp[Y_0|\epsilon|^{\psi\nu}H^{-2\psi/(d-2\theta)}/k_BT_g], \qquad (6)$$

just below T_g, where θ is the energy exponent. The equivalence of Eqs. (5) and (6) leads to the relation $\nu=(\beta+\gamma)/(d-2\theta)$. Since $\beta+\gamma=\nu(d-2\theta)=2-\alpha-2\nu\theta=2\beta+\gamma-2\nu\theta$, we obtain a scaling relation $(\beta=2\nu\theta)$. Then

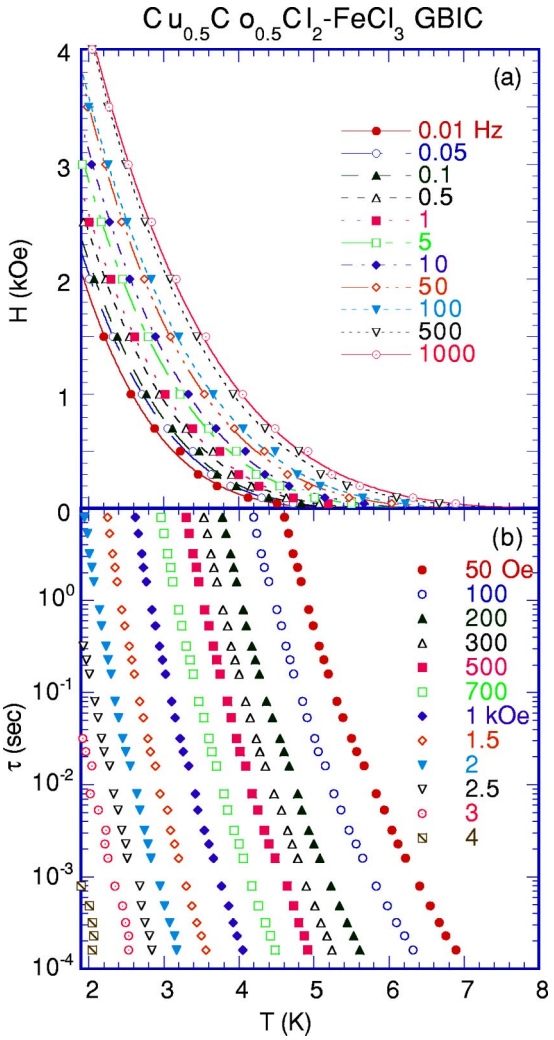

FIG. 12. (a) $T_f(H,\omega)$ contours at various H between $f=0.01$ Hz and 1 kHz, which is determined from Fig. 11. (b) τ vs T at various H, which is derived from (a). The lines are guides to the eyes.

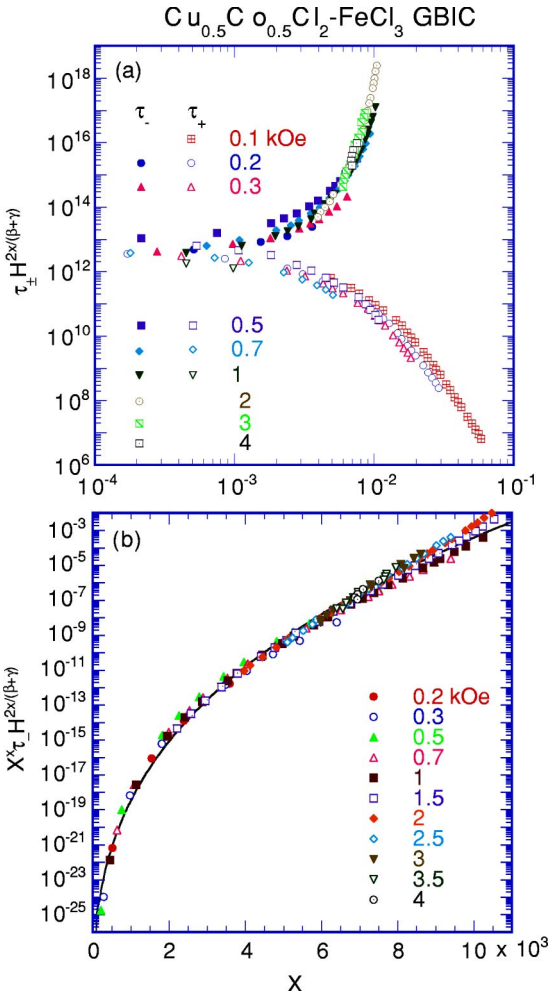

FIG. 13. (a) Scaling plot of $\tau_{\pm}H^{2x/(\beta+\gamma)}$ vs X at various H, where $X=|\epsilon|H^{-2/(\beta+\gamma)}$. The values of exponents β, γ, and x are given in the text. (b) Scaling plot of $X^x\,\tau_- H^{2x/(\beta+\gamma)}$ vs X at various H. The solid line is a fitting curve (see the text for detail).

$F_-(X)$ in Eq. (5) has the asymptotic form of $F_-(X)\approx\exp(X^{\psi\nu})$, since $Y_0/(k_BT_g)\approx 1$.

Our result of $\tau(T,H)$ shown in Fig. 12(b) is analyzed using the dynamic scaling relation. The relaxation time $\tau(T=T_g,H)$ is predicted to be proportional to $H^{-2x/(\beta+\gamma)}$ as $H\to 0$. In fact, the least squares fit of the data of τ vs H at $T_g=3.92$ K for $0.1\leqslant H\leqslant 1$ kOe yields the parameters $2x/(\beta+\gamma)=5.30\pm 0.13$. Since $x=10.3\pm 0.7$ and $\beta=0.36\pm 0.03$, the exponent γ is estimated as $\gamma=3.5\pm 0.4$. Using the scaling relations ($\alpha+2\beta+\gamma=2$ and $2-\alpha=d\nu$), the exponents α and ν are calculated as $\alpha=-2.2\pm 0.5$ and $\nu=1.4\pm 0.2$, where $d=3$. The exponent z is given by $z=6.6\pm 1.2$. These results agree with those predicted from the MC simulation by Ogielski for the 3D $\pm J$ Ising model ($\alpha=-1.9\pm 0.3$, $\beta=0.5$, $\gamma=2.9\pm 0.3$, $\nu=1.3\pm 0.1$, $z=6.0\pm 0.5$).[20] The exponent θ is estimated as $\theta=0.13\pm 0.02$ using the scaling relation ($\theta=\beta/2\nu$). The validity of this θ will be discussed in Sec. IV.

Figure 13(a) shows a scaling plot of $\tau_{\pm}(T,H)H^{2x/(\beta+\gamma)}$ a function of X,

$$\tau_{\pm}(T,H)H^{2x/(\beta+\gamma)}=G_{\pm}(X), \tag{7}$$

where $x=10.3$, $T_g=3.92$ K, $\beta=0.36$, and $\gamma=3.5$. We find that almost all the data fall well on two scaling functions: G_+ for $T>T_g$ and G_- for $T<T_g$. The scaling function $F_{\pm}$ is related to the scaling function $G_{\pm}$ by $F_{\pm}(X)=X^xG_{\pm}(X)$ with $x=10.3$. In Fig. 13(b) we show the plot of $F_{\pm}(X)$ as a function of X. The form of $F_-(X)$ is given as follows: $\ln[F_-(X)]=c_1X^{\psi\nu}+c_2$ with $c_1=300\pm 18$, $c_2=-72\pm 2$, and $\psi\nu=0.33\pm 0.01$. This fitting curve is determined from the data of τ_- at $H=3$ kOe. Since $\nu=1.4\pm 0.2$, ψ is estimated as 0.24 ± 0.02.

F. Possibility of SG phase transition at finite H

We consider the possibility that $\tau(T,H)$ may be described by a critical slowing down given by

$$\tau(T,H)=\tau^*[T/T_f(H)-1]^{-x} \tag{8}$$

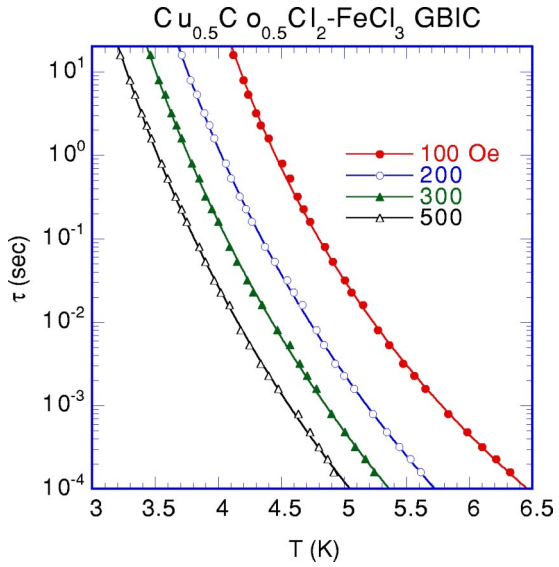

FIG. 14. Plot of τ vs T obtained from the data of $T_f(H,\omega)$ with $H=100$, 200, 300, and 500 Oe. The relaxation time τ is defined as $\omega\tau=1$ at $T=T_f(H,\omega)$.

for $T>T_f(H)$. This is based on the assumption that the SG transition is not destroyed by the application of H (the molecular field picture). The SG phase exists below $T_f(H)$ in thermal equilibrium. The least squares fits of the data of $\tau(T,H)$ vs T shown in Fig. 14 to the above power-law form yield $x=10.2\pm0.3$, $T_f(H)=3.10\pm0.05$ K, $\tau^*=2.3\times10^{-4}$ sec at $H=100$ Oe; $x=13.2\pm0.4$, $T_f(H)=2.35\pm0.07$ K, $\tau^*=1.2\times10^{-2}$ sec at $H=200$ Oe; $x=13.8\pm0.5$, $T_f(H)=2.08\pm0.08$ K, $\tau^*=5.2\times10^{-2}$ sec at $H=300$ Oe; and $x=13.6\pm0.6$, $T_f(H)=1.94\pm0.08$ K, $\tau^*=6.0\times10^{-2}$ sec at $H=500$ Oe. The values of $T_f(H)$ thus obtained are plotted as a function of H in Fig. 8. This line does not coincide with the line $T_f(H)$ determined form the local minimum temperature of $d\delta/dT$ vs T. These two lines start to deviate at $H\approx0$ Oe. The exponent x is strongly dependent on H. The value of x at $H=100$ Oe is almost equal to x at $H=0$, but it drastically increases with increasing H for $H\geqslant200$ Oe. These results suggest that the SG transition at $H=0$ is destroyed by the application of H (at least above 100 Oe). This result is consistent with the following theoretical prediction proposed by Lamarcq *et al.*[28] For $H<H_0$ (some characteristic field) the system behaves qualitatively just as in the case $H=0$, while significant changes arise for $H>H_0$. Our result is slightly different from the conclusion derived by Mattsson *et al.*[9] that the SG phase is destroyed at finite H for $Fe_{0.5}Mn_{0.5}TiO_3$. Note that there are some recent theories[29] supporting the result of Mattsson *et al.*

G. Aging at constant temperature

We have measured the t dependence of χ'' at $T=3.25$, 3.50, 3.75, 3.90, and 4.4 K, where $H=0$. The system was quenched from 10 K to T ($<T_g$) at time (age) zero. Both χ' and χ'' were measured simultaneously as a function of time t at constant T. Each point consists in the successive measurements of five frequencies ($f=0.05$, 0.1, 0.5, 1, and 5 Hz).

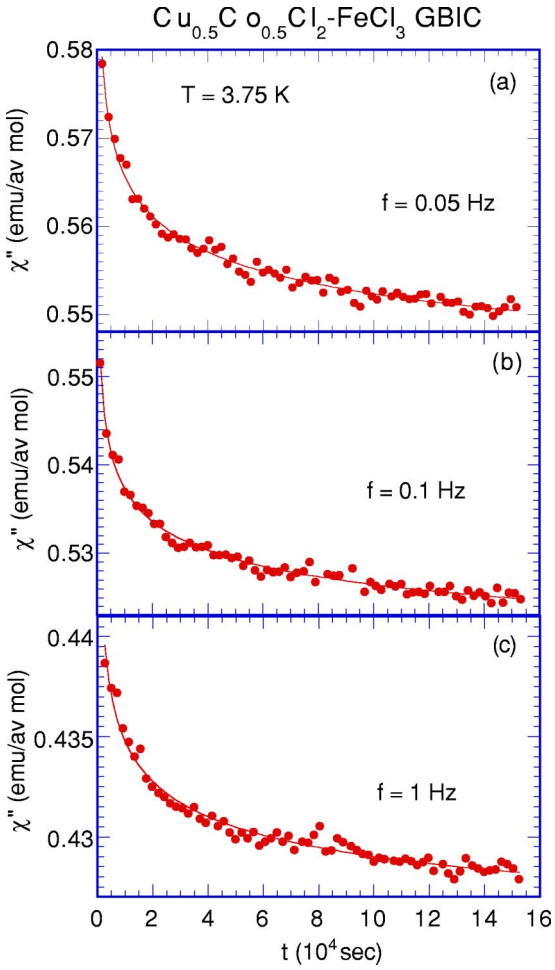

FIG. 15. t dependence of χ'' at $T=3.75$ K for $f=0.05$, 0.1, and 1 Hz, where t is the time taken after the sample was quenched from 50 to 3.75 K. The solid lines are the fits of the data to the power-law form.

Figure 15 shows the t dependence of χ'' at $T=3.75$ K for $f=0.05$, 0.1, and 1 Hz. The absorption χ'' decreases with increasing T and is well described by a power-law decay

$$\chi''(\omega,t)=\chi_0''(\omega)+A''(\omega)t^{-b''}. \tag{9}$$

The least squares fit of the data of $\chi''(\omega,t)$ at $T=3.75$ K to Eq. (9) yields fitting parameters listed in Table I. The exponent b'' is slightly dependent on f. The f dependence of the amplitude $A''(\omega)$ for $0.05\leqslant f\leqslant1$ Hz is described by $A''(\omega)=A_0''\omega^{-\mu''}$ with $A_0''=0.142\pm0.002$ and $\mu''=0.225\pm0.016$. The value of μ'' is almost the same as that of b'', supporting a ωt-scaling relation that Eq. (9) can be rewritten as

$$\chi''(\omega,t)=\chi_0''(\omega)+A_0''(\omega t)^{-b''}. \tag{10}$$

In Fig. 16(a) we show a scaling plot of $\Delta\chi''(\omega,t)$ at 3.75 K as a function of ωt, where $\Delta\chi''(\omega,t)=\chi''(\omega,t)-\langle\chi_0''(\omega)\rangle$. The stationary susceptibility $\langle\chi_0''(\omega)\rangle$ listed in Table I is slightly different from $\chi_0''(\omega)$ and corresponds to the asymptotic f-dependent value so that $\chi''(\omega,t)$ tends to zero in the limit of $t\to\infty$. Almost all the data fall well on a single

TABLE I. Fit parameters for the decay of χ'' vs t. $T=3.75$ K to Eq. (9). The definition of the parameters is given in the text.

f (Hz)	b''	$\chi_0''(\omega)$ (emu/av mol)	$\langle\chi_0''(\omega)\rangle$	$A''(\omega)$
0.05	0.159 ± 0.022	0.522 ± 0.005	0.535	0.188 ± 0.016
0.1	0.158 ± 0.019	0.502 ± 0.004	0.512	0.152 ± 0.010
0.5	0.185 ± 0.021	0.445 ± 0.002	0.449	0.111 ± 0.010
1	0.193 ± 0.033	0.419 ± 0.002	0.420	0.095 ± 0.016

scaling function given by Eq. (10) with $b''=\langle b''\rangle=0.255\pm0.005$ and $A_0''=\langle A_0''\rangle=0.239\pm0.009$. The value of $\langle b''\rangle$ is a little larger than that of b'' determined using the data at $f=0.05$ Hz. Note that $\langle b''\rangle$ is equal to 0.14 ± 0.03 at 19 K for $Fe_{0.5}Mn_{0.5}TiO_3$ ($T_g=20.7$ K).[30] The susceptibility $\langle\chi_0''(\omega)\rangle$ clearly decreases with increasing ω, which is consistent with the prediction by Picco *et al.*[31]

In Fig. 16(b) we show a scaling plot of $\Delta\chi'(\omega,t)$ at $T=3.75$ K, where $\Delta\chi'(\omega,t)=\chi'(\omega,t)-\langle\chi_0'(\omega)\rangle$ and

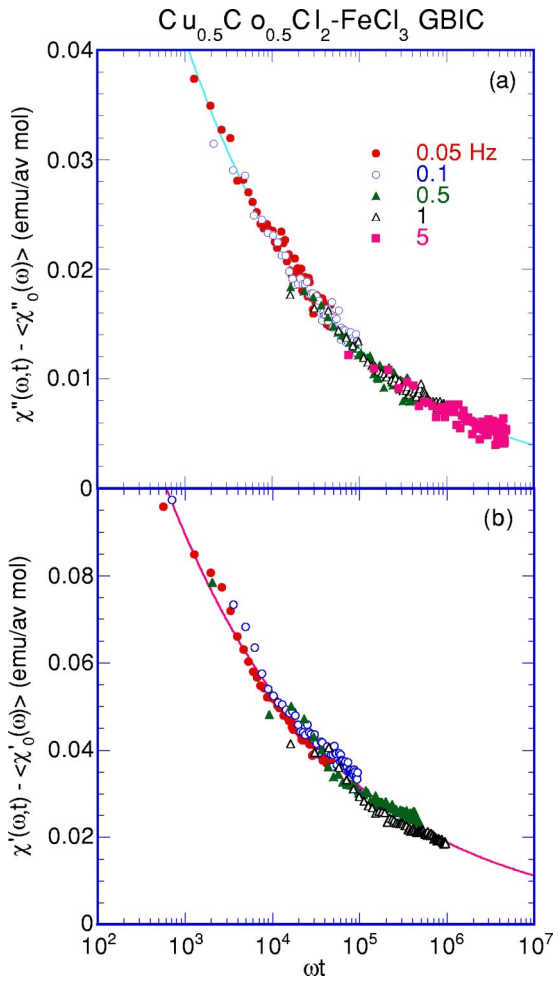

FIG. 16. Scaling plot of (a) $\Delta\chi''(\omega,t)[=\chi''(\omega,t)-\langle\chi_0''(\omega)\rangle]$ and (b) $\Delta\chi'(\omega,t)[=\chi'(\omega,t)-\langle\chi_0'(\omega)\rangle]$ as a function of ωt for the data at $f=0.05$, 0.1, 0.5, 1, and 5 Hz. The definition of stationary susceptibility $\langle\chi_0''(\omega)\rangle$ and $\langle\chi_0'(\omega)\rangle$ is given in the text. The solid lines are the fits of the data to the power-law form. Each curve is vertically shifted by $\langle\chi_0''(\omega)\rangle$ or $\langle\chi_0'(\omega)\rangle$ (see text for definition).

$\langle\chi_0'(\omega)\rangle$ is the stationary part of $\chi'(\omega,t)$ in the limit of $t\to\infty$. All the data lie well with a universal curve described by $\Delta\chi'(\omega,t)=A_0'(\omega t)^{-b'}$ with $b'=\langle b'\rangle=0.226\pm0.007$ and $A_0'=0.426\pm0.018$. The exponent $\langle b'\rangle$ is nearly equal to $\langle b''\rangle$. The susceptibility $\langle\chi_0'(\omega)\rangle$ decreases with increasing f, which is similar to the case of $\langle\chi_0''(\omega)\rangle$.

Such a power-law decay of $\chi''(\omega,t)$ and $\chi'(\omega,t)$ with t is observed only for 3.25 K $\leqslant T\leqslant T_g$. In Fig. 17 we shows the T dependence of b' and b'' at $f=0.05$ Hz. Both b' and b'' are of the same order at the same T. There is a steplike increase in b' and b'' with increasing T between 3.5 and 3.75 K; $b''=0.017\pm0.032$ at 3.50 K and $b''=0.16\pm0.04$ at 3.9 K just below T_g. Similar behavior on the T dependence of b'' has been reported by Colla *et al.*[32] for a relaxor ferroelectric $Pb(Mg_{1/3}Nb_{2/3})O_3$, which is not a SG system. We note that as shown in Fig. 2(b), the data of $d\delta/dT$ vs T for $H=1$ Oe exhibits a local minimum at 3.5 K, close to a temperature at which b'' undergoes a drastic increase.

H. Rejuvenation effect under perturbations

We also examine the aging effect of χ'' under perturbations such as the change of T and H. Figure 18 shows the t dependence of $\chi''(\omega,t)$ under a negative temperature cycle, where $f=0.05$ Hz and $h=0.1$ Oe. Here our system was quenched from $T=10$ to 3.75 K at $H=0$. The relaxation of

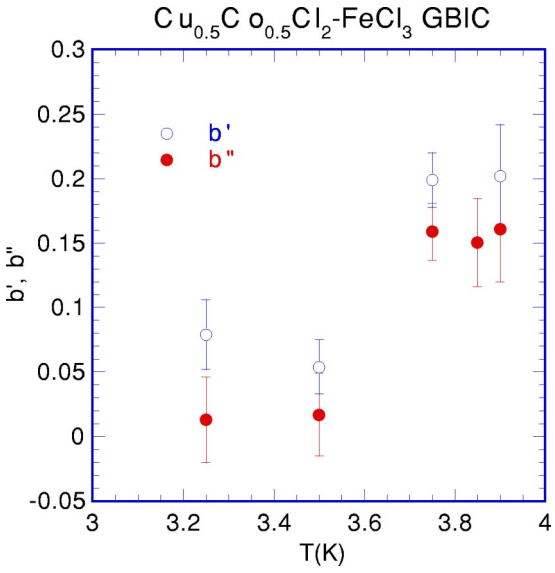

FIG. 17. T dependence of exponents b' and b''.

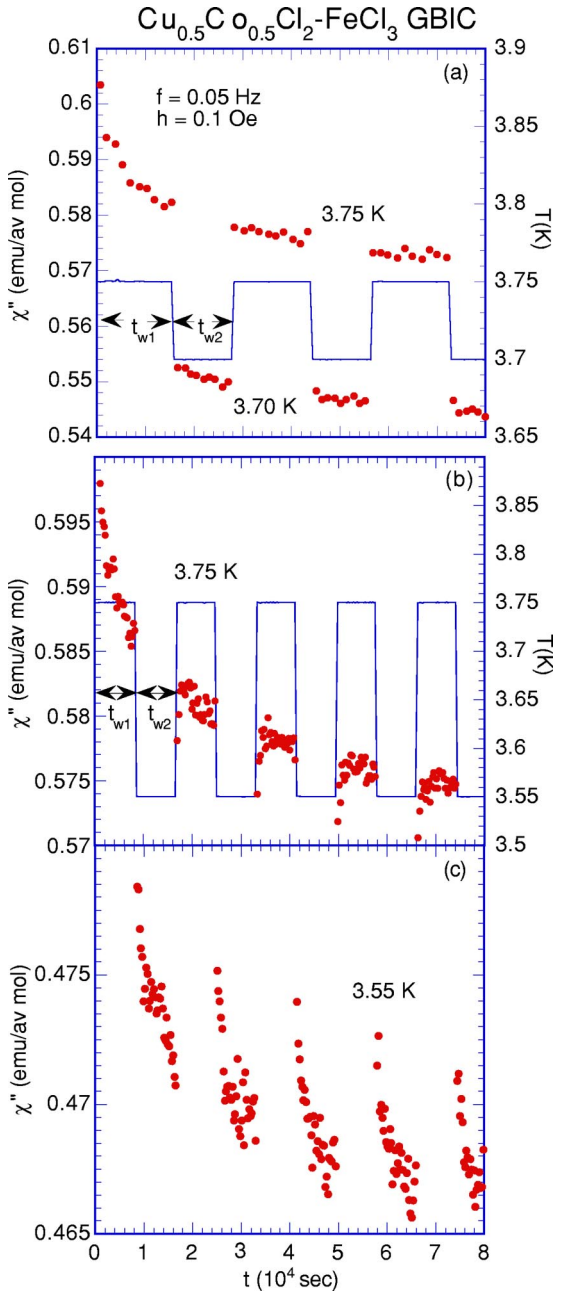

FIG. 18. Relaxation of $\chi''(\omega,t)$ during a negative temperature cycle. $f=0.05$ Hz, $T=3.75$ K, and $T-\Delta T$. $H=0$. The change of T with t is also shown. (a) $\Delta T=0.05$ K. (b) and (c) $\Delta T=0.20$ K.

$\chi''(\omega,t)$ was measured as a function of t during a period t_{w1} ($\approx 1.5\times 10^4$ sec). The temperature was then changed to $T-\Delta T$ (the first T-shift). The relaxation of χ'' was measured as a function of t for a period t_{w2} ($\approx 1.5\times 10^4$ sec) at $T-\Delta T$. The system was again heated back to T (the second T-shift). These processes were repeated subsequently. In the case of $\Delta T=0.05$ K [Fig. 18(a)], just after the first T-shift χ'' behaves as if the system were quenched to $T-\Delta T$ directly from 10 K. After the second T-shift, however, $\chi''(\omega,t)$ coincides with a simple extension of $\chi''(\omega,t)$ already aged by t_{w1} at T. In the case of $\Delta T=0.20$ K [Figs. 18(b) and 18(c)], χ'' undergoes a drastic change to a value higher than the value just before the change of T from 3.55 to 3.75 K, when T is changed from 3.75 to 3.55 K. Then the relaxation of χ'' newly occurs (the rejuvenation effect).

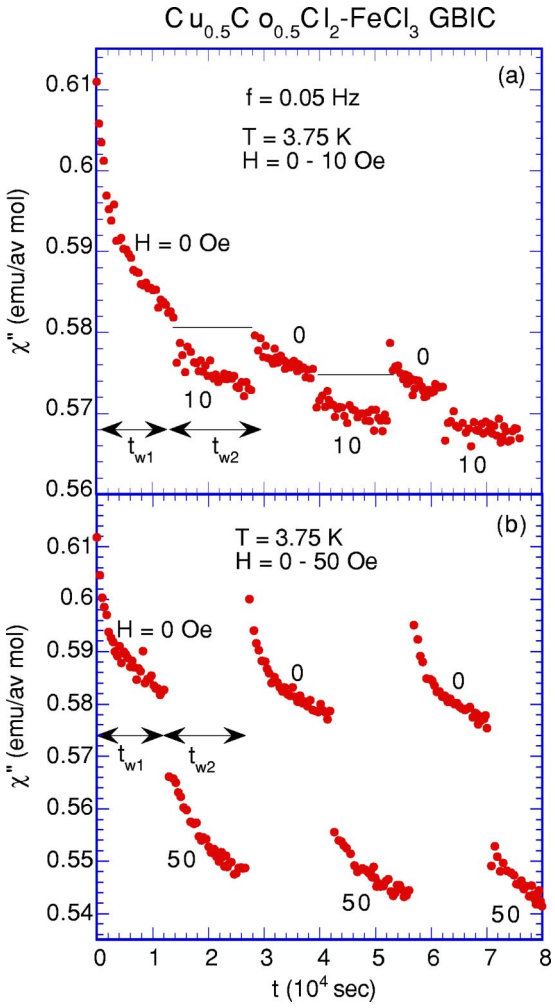

FIG. 19. Relaxation of $\chi''(\omega,t)$ during a magnetic field cycling. $f=0.05$ Hz, $T=3.75$ K. (a) $H=0$ and 10 Oe. (b) $H=0$ and 50 Oe.

Figure 19 shows the t dependence of $\chi''(\omega,t)$ at $T=3.75$ K under a positive H cycle, where $f=0.05$ Hz and $h=0.1$ Oe. In these measurements, the system was cooled down to 3.75 K at $H=0$. The relaxation of χ'' was measured as a function of t during a period t_{w1}. A magnetic field H ($=10$ and 50 Oe) was then applied at $t=t_{w1}$. The relaxation of χ'' was measured as a function of t for a period t_{w2} at H. The field H was again reduced to zero. The relaxation of χ'' was measured as a function of t at $H=0$. These processes were repeated. In the case of $H=10$ Oe [Fig. 19(a)], when the field is off from 10 to 0 Oe, χ'' rises to a value of χ'' to which χ'' is supposed to decay during the period t_{w2} at $H=0$. In the case of $H=50$ Oe [Fig. 19(b)], χ'' undergoes a drastic change to a value higher than the value just before the change of H from 0 to 50 Oe, when the field is off from 50 to 0 Oe. Then the relaxation of χ'' newly occurs (the rejuvenation effect). This effect is similar to those reported in $Fe_{0.5}Mn_{0.5}TiO_3$ (Refs. 30 and 33) and $CdCr_{1.7}In_{0.3}S_4$.[30]

IV. DISCUSSION AND CONCLUSION

In this paper we study the nature of the slow dynamics of the short-range Ising SG, $Cu_{0.5}Co_{0.5}Cl_2$-$FeCl_3$ GBIC. Using the concepts of static and dynamic scaling laws, we determine the critical exponents of this compound. Our results are as follows: $\alpha=-2.2\pm0.5$, $\beta=0.36\pm0.03$, $\gamma=3.5\pm0.4$, $\nu=1.4\pm0.2$, $\eta=-0.5\pm0.2$, $z=6.6\pm1.2$, $\phi=3.9\pm0.4$, $\theta=0.13\pm0.02$, and $\psi=0.24\pm0.02$, where $2-\eta=\gamma/\nu$. These critical exponents are compared with those reported for the Ising SG, $Fe_{0.5}Mn_{0.5}TiO_3$ ($\alpha=-3$, $\beta=0.5\pm0.2$, $\gamma=4.0\pm0.4$, $\nu=1.7$, $z=6.2$, $\phi=4.5$, $\theta\approx0.2$, and $\psi=0.3$–0.7) (Refs. 19, 25, 30, and 33) and Heisenberg-like SG, $CdCr_{1.7}In_{0.3}S_4$ ($\alpha=-1.9$, $\beta=0.75\pm0.1$, $\gamma=2.3\pm0.4$, $\nu=1.26\pm0.2$, $\phi=3.1\pm0.5$, $z\nu=7$, $\psi=1.1$).[30,34] Our critical exponents are in excellent agreement with those of amorphous metallic SG, $(Fe_{0.15}Ni_{0.85})_{75}P_{16}B_6Al_3$ ($\alpha=-2.2$, $\beta=0.38$, $\gamma=3.4$, $\nu=1.39$, $z=5.9$).[35,36] Note that we use the scaling relation given by $\beta=2\theta\nu$ to determine θ of our system. This relation is derived in the present work using the idea of dynamic scaling law for the T and H dependence of τ_-. This relation is valid for $Fe_{0.5}Mn_{0.5}TiO_3$: the value of $\theta(=\beta/2\nu=0.15)$ is close to the experimental value ($\theta\approx0.2$). We note that a relation $(1=2\nu\theta)$ is derived by Fisher and Huse[5] in the case of $d\rightarrow d_l^+$. Here d_l^+ is the lowest dimension where $\theta>0$ and d_l^+ is close to 2.5.[37] If β is equal to the mean-field exponent ($\beta=1$), then the scaling relation ($\beta=2\nu\theta$) coincides with the relation derived by Fisher and Huse.[5]

Our value of θ is a little smaller than the theoretical values: $\theta=0.19\pm0.01$ by Bray and Moore,[6] $\theta=0.192\pm0.001$ by Hartmann,[38] and $\theta=0.20\pm0.03$ by Komori *et al.*[39] from MC simulations on the relaxation of energy of the 3D Gaussian SG model with nearest neighbor interactions. Our value of ψ is a little larger than that of θ, satisfying the imposed inequality $\theta\leqslant\psi\leqslant(d-1)$.[5] This condition is also satisfied in the other SG systems: $Fe_{0.5}Mn_{0.5}TiO_3$ ($\psi=0.3$–0.7) (Ref. 30) and $CdCr_{1.7}In_{0.3}S_4$ ($\psi=1.1$).[30] The value of ψ is strongly dependent on the spin symmetry (n) of the systems such as Ising ($n=1$) and Heisenberg ($n=3$): it decreases as the spin symmetry n decreases. This is also true for the critical exponent β: β decreases with decreasing n.[37] The small values of ψ and β indicates that our system magnetically behaves like an ideal 3D short-range Ising SG.

Finally we discuss the T dependence of b''. The exponent b'' is dependent on T. According to Komori *et al.*,[40] the ratio $\Delta\chi''(\omega,t)/\chi'(\omega)$ is described by

$$\Delta\chi''(\omega,t)/\chi''(\omega)\approx(\omega t)^{-b''(T)}, \tag{11}$$

where $b''(T)=(d-\theta)/z(T)$ and the exponent $1/z(T)$ is linearly dependent on T well below T_g: $1/z(T)=T/(zT_g)$. This ωt scaling of $\Delta\chi''(\omega,t)/\chi''(\omega)$ is derived on the assumption that the growth law of the spin-glass correlation length $\xi(t)$ is approximated by the form $\xi(t)\approx l_0(t/t_0)^{1/z(T)}$, where l_0 and t_0 are microscopic length and time scales. This growth law is different from that proposed in the scaling picture due to Fisher and Huse.[4] Using the values of θ and $b''(T)$, the exponent $1/z(T)$ is calculated as 0.006 at 3.50 K and 0.056 at 3.90 K. Such an increase of $1/z(T)$ with T qualitatively agrees with the prediction by Komori *et al.*[40] If the expression $1/z(T)=T/(zT_g)$ is valid at $T=3.90$ K just below T_g, the value of z can be estimated as 18, which is much larger than our value $z(=6.6)$. Experimentally $b''(T)$ is nearly equal to zero below ≈3 K ($\approx0.75T_g$). At present we give no satisfactory explanation for the cause of the drastic change in b'' around 3.5 K in our system.

In conclusion, we have shown that $Cu_{0.5}Co_{0.5}Cl_2$-$FeCl_3$ GBIC magnetically behaves like an ideal 3D short-range Ising SG. This compound undergoes a SG phase transition at $T_g=3.92\pm0.11$ K. The dynamic scaling analysis suggests that this SG transition is destroyed by the application of H (at least above 100 Oe). The scaling behavior of the relaxation time is well described by the scaling picture with the energy exponent $\theta=0.13\pm0.02$ and the barrier exponent $\psi=0.24\pm0.02$. The aging obeys the ωt scaling. The rejuvenation effect is observed under sufficiently large (temperature and magnetic-field) perturbations.

In spite of such a similarity in dynamic behaviors between $Cu_{0.5}Co_{0.5}Cl_2$-$FeCl_3$ GBIC and 3D Ising spin glass, the frequency dependence of χ'' below T_g are very different. The absorption χ'' in $Cu_{0.5}Co_{0.5}Cl_2$-$FeCl_3$ GBIC decreases with increasing frequency, whereas χ'' in 3D Ising spin glass increases with increasing frequency.

ACKNOWLEDGMENTS

We would like to thank H. Suematsu for providing us with single crystal kish graphite and T. Shima, B. Olson, and M. Johnson for their assistance in sample preparation and x-ray characterization. Early work, in particular for the sample preparation, was supported by NSF DMR Grant No. 9201656.

*Email address: itsuko@binghamton.edu
†Email address: suzuki@binghamton.edu

[1] E. Marinari, G. Parisi, and J.J. Ruiz-Lorenzo, in *Spin Glasses and Random Fields*, edited by A.P. Young (World Scientific, Singapore, 1998), p. 59. See also references therein.
[2] W.L. McMillan, J. Phys. C **17**, 3179 (1984).
[3] D.S. Fisher and D.A. Huse, Phys. Rev. Lett. **56**, 1601 (1986).
[4] D.S. Fisher and D.A. Huse, Phys. Rev. B **38**, 373 (1988).
[5] D.S. Fisher and D.A. Huse, Phys. Rev. B **38**, 386 (1988).
[6] A.J. Bray and M.A. Moore, Phys. Rev. Lett. **58**, 57 (1987).
[7] A.J. Bray, Comments Condens. Matter Phys. **14**, 21 (1988).
[8] J.R.L. de Almeida and D.J. Thouless, J. Phys. A **11**, 983 (1978).
[9] J. Mattsson, T. Jonsson, P. Nordblad, H.A. Katori, and A. Ito, Phys. Rev. Lett. **74**, 4305 (1995).
[10] P. Nordblad and P. Svedlindh, in *Spin Glasses and Random Fields* (Ref. 1), p. 1. See also references therein.
[11] D. Petit, L. Fruchter, and I.A. Campbell, Phys. Rev. Lett. **83**, 5130 (1999).
[12] I.S. Suzuki, M. Suzuki, H. Satoh, and T. Enoki, Solid State Commun. **104**, 581 (1997).

[13] M. Suzuki and I.S. Suzuki, Phys. Rev. B **59**, 4221 (1999).
[14] T. Enoki, M. Suzuki, and M. Endo, in *Graphite Intercalation Compounds and Applications* (Oxford Universitry Press, Oxford, 2003), p. 236.
[15] I.S. Suzuki and M. Suzuki, Solid State Commun. **106**, 513 (1998).
[16] I.S. Suzuki and M. Suzuki, J. Phys.: Condens. Matter **11**, 521 (1999).
[17] A. Ito, H. Aruga, E. Torikai, M. Kikuchi, Y. Syono, and H. Takei, Phys. Rev. Lett. **57**, 483 (1986).
[18] M.F. Hansen, P.E. Jönsson, P. Nordblad, and P. Svedlindh, J. Phys.: Condens. Matter **14**, 4901 (2002).
[19] K. Gunnarsson, P. Svedlindh, P. Nordblad, L. Lundgren, H. Aruga, and A. Ito, Phys. Rev. Lett. **61**, 754 (1988).
[20] A.T. Ogielski, Phys. Rev. B **32**, 7384 (1985).
[21] J.-P. Bouchaud, V. Dupuis, J. Hammann, and E. Vincent, Phys. Rev. B **65**, 024439 (2001).
[22] P. Svedlindh, K. Gunnarsson, P. Nordblad, L. Lundgren, H. Aruga, and A. Ito, Phys. Rev. B **40**, 7162 (1989).
[23] C.C. Paulsen, S.J. Williamson, and H. Maletta, Phys. Rev. Lett. **59**, 128 (1987).
[24] S. Geschwind, D.A. Huse, and G.E. Devlin, Phys. Rev. B **41**, 4854 (1990).
[25] K. Gunnarsson, P. Svedlindh, P. Nordblad, L. Lundgren, H.A. Katori, and A. Ito, Phys. Rev. B **43**, 8199 (1991).
[26] H.A. Katori and A. Ito, J. Phys. Soc. Jpn. **63**, 3122 (1994).
[27] K.H. Fischer and J.A. Hertz, *Spin Glasses* (Cambridge University Press, Cambridge, 1991), p. 263.
[28] J. Lamarcq, J.-P. Bouchaud, and O.C. Martin, Phys. Rev. B **68**, 012404 (2003).
[29] J. Houdayer and O.C. Martin, Phys. Rev. Lett. **82**, 4934 (1999). See also references therein.
[30] V. Dupuis, E. Vincent, J.-P. Bouchaud, J. Hammann, A. Ito, and H.A. Katori, Phys. Rev. B **64**, 174204 (2001).
[31] M. Picco, F. Ricci-Tersenghi, and F. Ritort, Eur. Phys. J. B **21**, 211 (2001).
[32] E.V. Colla, L.K. Chao, M.B. Weissman, and D.D. Viehland, Phys. Rev. Lett. **85**, 3033 (2000).
[33] P.E. Jönsson, H. Yoshino, P. Nordblad, H.A. Katori, and A. Ito, Phys. Rev. Lett. **88**, 257204 (2002).
[34] E. Vincent and J. Hammann, J. Phys. C **20**, 2659 (1987).
[35] L. Lundgren, P. Nordblad, and P. Svedlindh, Phys. Rev. B **34**, 8164 (1986).
[36] P. Svedlindh, L. Lundgren, P. Nordblad, and H.S. Chen, Europhys. Lett. **3**, 243 (1987).
[37] I.A. Campbell, D. Petit, P.O. Mari, and L.W. Bernardi, J. Phys. Soc. Jpn. **69**, Suppl. A, 186 (2000).
[38] A.K. Hartmann, Phys. Rev. E **59**, 84 (1999).
[39] T. Komori, H. Yoshino, and H. Takayama, J. Phys. Soc. Jpn. **68**, 3387 (1999).
[40] T. Komori, H. Yoshino, and H. Takayama, J. Phys. Soc. Jpn. **69**, 1192 (2000).